Structural Performance of a Reinforced Concrete Double-Beam System

Jae-Man Lee, Senior Researcher, Lotte Eng. and Construction, Seoul, South Korea; **Yong-Jun Lee,** PhD Candidate, Kongju National Univ., Cheonan, South Korea; **Sang-Woo Kim,** Research Asst. Prof., Kongju National Univ., Cheonan, Republic of Korea; **Kwang-Man Kim,** CEO and Pres., Baro Construction and Eng., Seoul; Republic of Korea; **Jung-Yoon Lee,** Prof., Sungkyunkwan Univ., Suwon, Republic of Korea; **Kil-Hee Kim,** Prof., Kongju National Univ., Chungnam, South Korea. Contact: kimkh@kongju.ac.kr
DOI: 10.2749/101686616X14555428758803

Abstract

A new reinforced concrete (RC) structural system suitable for long-span structures was developed. The system consists of a slab, a column, double beams and a drop panel. To investigate the structural performance of the system, four specimens of 30% scale were constructed and tested. Using two experimental parameters, the number of longitudinal bars in the beam and drop panel, and the effect of the parameters on the structural behaviour of the system were scrutinized. All four specimens showed satisfactory allowable deflection of *l*/480 as allowed in design code of American Concrete Institute (ACI318-11). The inclusion of the drop panel in the proposed system reduced the negative moment in the column zone and contributed to the realization of deflection control. The proposed system was found to be effective for the realization of long-span structures that are also easy to build. The advantages of the proposed system in terms of economic efficiency were revealed by cost analysis of a conventional RC system and the proposed system. Compared with the conventional RC system, an approximately 25% cost-saving effect was achieved for the proposed system.

Keywords: reinforced concrete; long-span structure; drop panel; reduction of deflection; negative moment; amount of rebar.

Introduction

In order to meet the recent requirements of the construction industry, such as reduction in the construction period and rationalization of construction technologies, development of rational long-span structures is essential. In previous research[1–7] it has been shown that the development of a rational long-span structure will be one of the most important issues that will need to be addressed to achieve savings in construction costs and effective usage of inner spaces of public facilities such as parking lots. For the realization of a long-span structural system, increases in deflection with increase in member length should be prevented appropriately. Development of long-span members (over 13 m length minimum) with new structural materials and state of the art structural engineering technologies is therefore required in order to achieve a long-span structural system.

Peer-reviewed by international experts and accepted for publication by SEI Editorial Board

Paper received: March 31, 2015
Paper accepted: December 14, 2015

Several achievements have been made in former studies towards the development of a long-span structural system. Steel and prestressed concrete structures have been the alternatives to long-span structures for a long time. A number of structural systems for long-span structures, such as S-SRC bars, eco-prestressed concrete beams, the TSC method, have been developed,[8] as shown in *Fig. 1*. The S-SRC bar system (*Fig. 1a*), consisting of steel girders and Z-shaped steel plates filled with concrete, reduces the sectional depth of steel girders. Eco-prestressed concrete beam system (*Fig. 1b*), consisting of prestressed, precast concrete beams and steel columns, was developed to provide a system that is easy to build and can prevent members from cracking. The TSC (The SEN Steel Concrete) method (*Fig. 1c*), which utilizes U-shaped steel girders and concrete, was developed to improve the weak flexural rigidity of steel girders. In this method a T-shaped gravity load-resisting system in which a steel girder is filled with concrete is integrated with a concrete slab. However, as the structural systems mentioned above do have limits in terms of construction cost and building techniques, they have not been aggressively applied to practical construction.

In order to develop a structural system that is economical and easy to build, a new structural system known as the double-beam system (DBS) (shown in *Fig. 1d*) was proposed. The system consists of a slab, a column, a drop panel and double beams. The drop panel is formed by double reinforced concrete (RC) beams adjacent and penetrating to the top of the column. The general distribution of the bending moment is indicated in *Fig. 2*. Reduction of the span length and negative moment in the column zone can be achieved in this system, as shown in *Fig. 2*. These factors will lead to a reduction in the deflection and help in completion of the long-span structure. Also, effective redistribution of the moment from the beam to the drop panel is facilitated. To quantitatively study the structural performance of the system, four RC specimens with double reinforced concrete beams and a drop panel were constructed and tested on Feb. to July, 2014. This paper will discuss the experimental results obtained from the test of the new structural system proposed in this study. As the proposed structural system covers the reduction in the deflection of underground structures or the lower portion of buildings such as parking lots, the structural characteristics of the specimens with regard to gravity load will be scrutinized. The economic efficiency of the system (analysis of cost) will also be discussed by comparing this system with the conventional RC structural system. Other performances such as floor vibration or fire-resistance properties of the proposed system will be covered in follow-up research.

Structural Performance

Design and Construction of the Specimens

Four specimens of 30% scale were constructed for testing. The number of longitudinal bars in the drop panel and

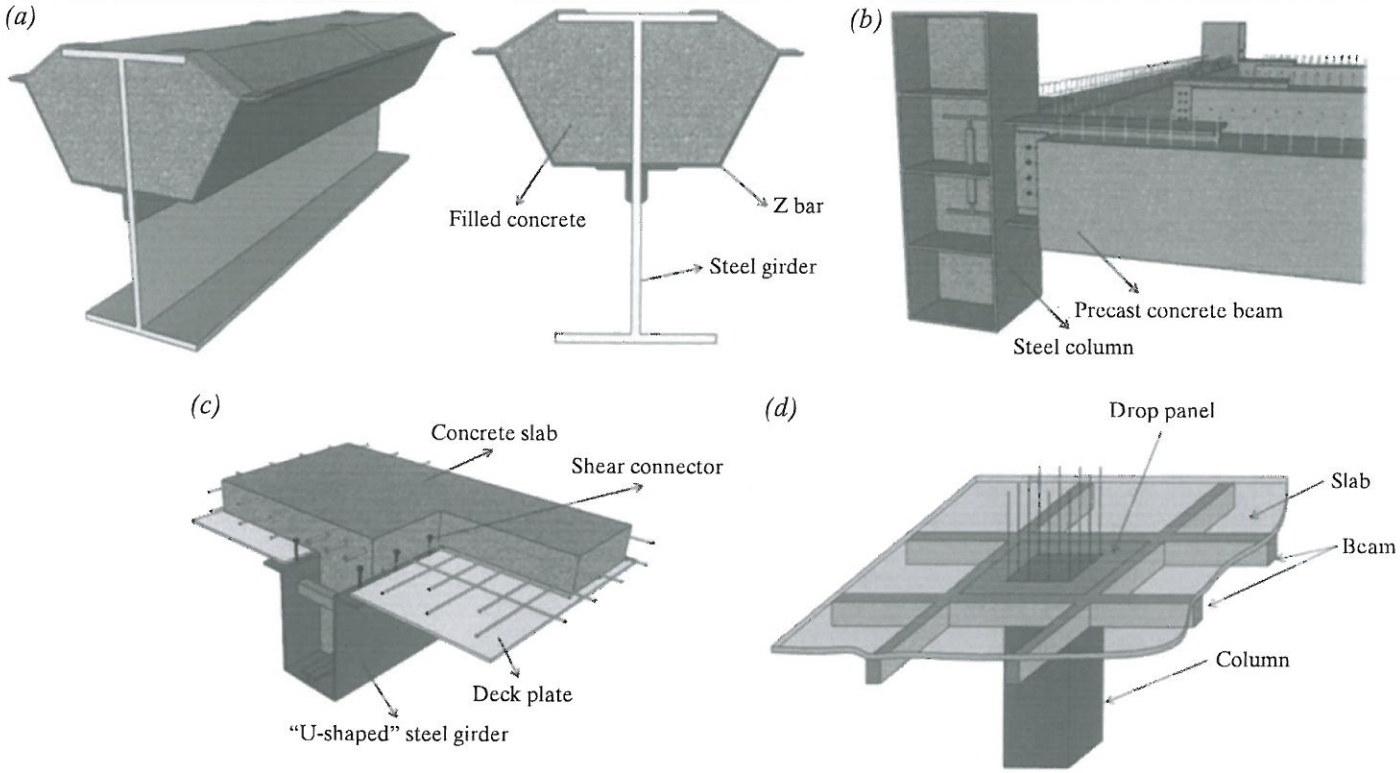

Fig. 1: The structural system. (a) S-SRC bar; (b) eco-prestressed concrete beams; (c) TSC method; (d) proposed system (DBS)

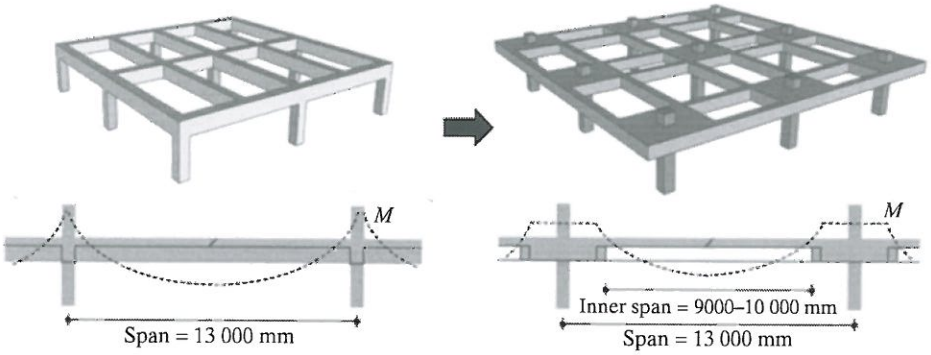

Fig. 2: Reduction of negative moment by DBS

beams, A_{rd} and A_{rb}, were selected as the experimental parameters. *Figure 3* provides an illustration of the section, the reinforcement details and the loading set-up of a specimen. The specimens are made of slab, double beams, columns and a drop panel zone. As can be seen in the figure, each specimen was constructed using two-bay continuous beams and a drop panel. The length and cross-sectional dimensions of the beam are 5000 mm and 150 × 200 mm, respectively. The volumetric size of the drop panel is 1350 × 900 × 200 mm. Beams in all specimens were designed to fail in flexure prior to shear. Also, they were designed such that punching shear failure of drop panel zones does not occur prior to flexural yielding. *Table 1* summarizes the main specifications and the experimental parameters allocated to each specimen. *Table 2* summarizes the mechanical properties of the materials used in each specimen.

A software package for finite element analysis was used in the design of the standard specimen.[9] The A_{rd} estimation used in the design of the standard specimens (DBS 1) made it possible for the system to resist the maximum tensile stress in the drop panel section, which was obtained by finite element analysis (*Fig. 3*, A_{rd} = 856.0 mm^2). Higher A_{rd} value was applied to DBS 2 and DBS 3 (A_{rd} = 1520.4 mm^2) to investigate the effect of a "stiff drop panel" on the structural behaviour of the proposed system. In DBS 4, in order to consider the possibility of an economical design, longitudinal bars that were less than 40% of A_{rd} in DBS 1 were applied (A_{rd} = 499.3 mm^2). To arrive at the number of longitudinal bars in a beam, A_{rb}, two longitudinal reinforcements (2-D13) were arranged in the tension zones of DBS 1, DBS 2 and DBS 4. For DBS 3, three longitudinal bars were arranged in the tension zone (3-D13). These arrangements result in A_{rb} value of 253.4 mm^2 for DBS 1, 2 and 4, and 380.1 mm^2 for DBS 3. Hence, M_d/M_b, where M_d and M_b indicate the flexural strength of the drop zone and beam, is equal to 3.33 for DBS 1, 5.19 for DBS 2, 3.68 for DBS 3 and 2.39 for DBS 4. By comparing DBS 2 with DBS 1, the effect of the stiff drop panel (with higher A_{rb}) on the structural performance of the system can be addressed. A comparison of DBS 3 with DBS 2 provides an investigation into the effect of the stiff beam (with higher A_{rb}) on the structural behaviour of the system. The comparison between DBS 1 and DBS 4 can provide information on the effect of the flexible drop panel on the structural behaviour of the system and indicate the possibility of an economical design via the reduction of the A_{rd} value in the system. The longitudinal bars arranged in the drop panel were anchored at 300 mm lengths into the slab. To prevent the beam from experiencing shear failure, the ratio of shear strength to the flexural strength was maintained at approximately 2.0. This results in a 60 mm pitch of the stirrups in the beam.

Loading and Measurements

Figure 3d illustrates the loading set-up for the specimens. The specimens have pin support at both the right and left ends and rigid support at the centre of the column. Using a hydraulic jack,

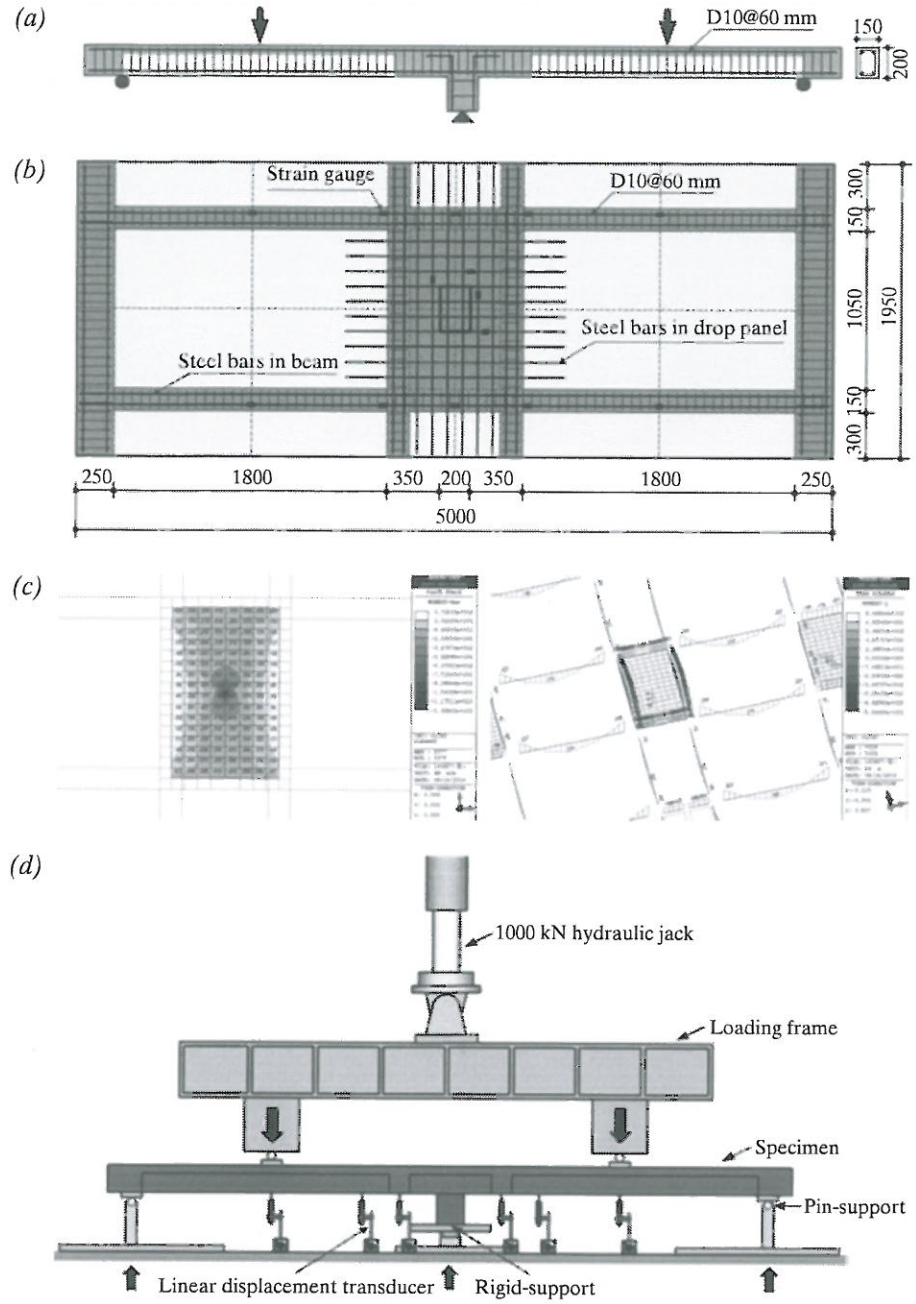

Fig. 3: Details and test set-up of specimen. (a) Front view; (b) plan; (c) assessment of the amount of rebar in drop panel of DBS1; (d) loading set-up

ramp loading was provided at mid-span of the left and right beams. The deflection values at mid-span of the beam, adjacent to the drop panel, and at a distance of one-fourth span from the centre of the column were measured using linear displacement transducers, as shown in the figure. The strain of the longitudinal bars and web reinforcements in the beams and the drop panel were measured using the strain gauges attached to each reinforcement. The load, deflection and strain were consecutively monitored and recorded. Crack patterns were first observed at primary cracking, Δ_{cr}. After that, crack patterns were observed at the deflection corresponding to the primary yielding of the longitudinal bar, Δ_y, and at deflections corresponding to $2\Delta_y$, $4\Delta_y$ and $6\Delta_y$. The test was terminated when the load-carrying capacity of the specimen dropped below 85% of the peak load.

Load–Deflection Relationship

The load–deflection relationships, V–Δ, of each specimen are plotted in *Fig. 4*. Horizontal and vertical axes represent the deflection and the load, respectively. Enlarged load–deflection curves until $\Delta = 6$ mm are also indicated in the figure. The deflection in the figure, Δ, represents the deflection at mid-span of a beam in which the tensile strain of the longitudinal bar first reached its yield strain. The symbols in *Fig. 4*, solid circles, open triangles, solid triangles and solid rectangles, indicate the points of initiation of flexural cracking, service load (SL), primary yielding of longitudinal bar in beam and maximum load-carrying capacity of the specimen, respectively. *Table 3* summarizes the experimental results, giving the values of Δ_s, V_s, Δ_y, V_y, Δ_u and V_u for each specimen. The notations Δ_s and V_s in the table represent the deflection and the load-carrying capacity of specimens at SL corresponding to tensile stress in longitudinal bars of $0.6f_y$, where f_y is the yield strength of the longitudinal bar in the beam. Also, Δ_y and V_y in the table indicate the deflection and load-carrying capacity of the specimen at primary yielding of the longitudinal bar in the beam, while Δ_u, and V_u represent the deflection and maximum load at the ultimate state.

Primary flexural cracks were initiated at approximately 60 kN in all specimens. In DBS 1, flexural yielding was observed at a deflection of 4.16 mm, corresponding to 160.5 kN. In DBS 2, load and deflection corresponding to Δ_y and V_y were 3.98 mm and 161.0 kN, respectively. Also, it should be noted that DBS 1 and DBS 2 reached their ultimate states at Δ_u = 295.5 and 275.5

Specimens	Specifications						Experimental parameters	
	Beam			Drop panel			Beam	Drop panel
	b (mm)	h (mm)	d (mm)	b (mm)	h (mm)	d (mm)	A_{rb} (mm^2)	A_{rd} (mm^2)
DBS 1	150	200	160	1350	200	160	253.4 (2-D13)	856.0 (D10@100mm)
DBS 2								1520.4 (D13@100mm)
DBS 3							380.1 (3-D13)	1520.4 (D13@100mm)
DBS 4							253.4 (2-D13)	499.3 (D10@150mm)

Table 1: Main specifications and experimental parameters

	Concrete*		Reinforcement					
			D10			D13		
	f_c (MPa)	E_c (GPa)	f_y (MPa)	f_u (MPa)	E_s (GPa)	f_y (MPa)	f_u (MPa)	E_s (GPa)
DBS 1	29.9	26.2	373.3	517.0	191.7	364.6	523.6	191.0
DBS 2								
DBS 3								
DBS 4	36.0	22.5	353.2	536.6	190.0	385.3	601.1	188.3

*Compressive strength tests of concrete were conducted using cylinder specimens.

Table 2: Mechanical properties of materials used in this study

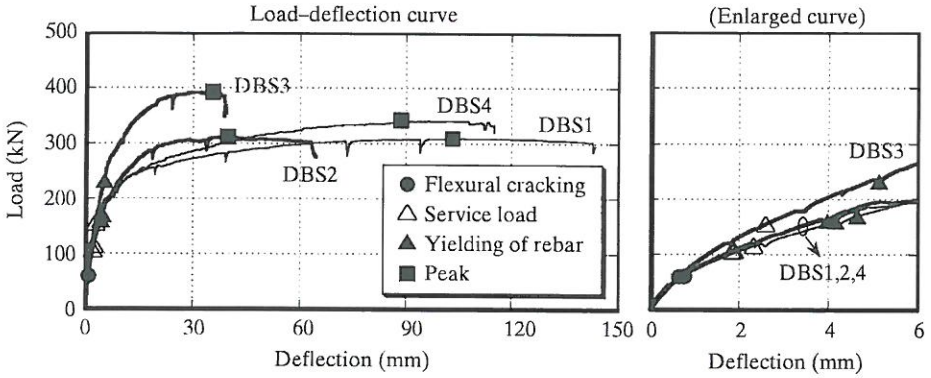

Fig. 4: Load–deflection relationships

	At service load		At yielding of reinforcement		At ultimate state (failure)	
	Δ_s (mm)	V_s (kN)	Δ_y (mm)	V_y (kN)	Δ_u (mm)	V_u (kN)
DBS 1	1.90	108.0	4.16	160.5	143.6	295.5
DBS 2	1.85	107.0	3.98	161.0	64.6	275.5
DBS 3	2.60	155.5	5.15	232.5	39.3	353.5
DBS 4	2.33	115.5	4.65	170.5	115.2	325.0

Table 3: Summary of experimental results

mm and DBS 1 was shown to be more ductile than DBS 2 in terms of the deformation capacity of the specimens. In DBS 3, Δ_u of 39.3 mm and V_u of 353.5 kN were observed. This indicates that the ultimate deformation capacity of DBS 3 was poorer than that of DBS 1, while the ultimate strength of DBS 3 was approximately 50 kN larger than that of DBS 1. As shown in *Fig. 4* and in *Table 3*, because the $6\Delta_y$ values of all specimens were in a range of approximately 23.9 to 27.9 mm, it can be seen that all specimens maintained their capacity until $\Delta = 6\Delta_y$. In summary, an increase in A_{rd} led to a decrease in the deformation capacity of the specimen. However, the observation that the Δ_u value of DBS 3 is also much greater than $6\Delta_y$ reveals that DBS 3 also behaved in a ductile manner. DBS 4 behaved in a manner similar to that of DBS 1 (Δ_y = 4.65 mm, V_y = 170.5 kN, Δ_u = 115.2 mm and V_y = 325.0 kN). From the above observations, it can be concluded that all specimens exhibited a ductile manner, and the value of A_{rd} adopted in the design of the specimens was appropriate.

Crack Patterns

Figure 5 illustrates the crack pattern of each specimen at the termination of the test. Primary flexural cracks were initiated at the mid-span of the beams in all specimens (dashed line in the figure). With the increasing of the load, the cracks propagated towards the compression fibres of the beams. Inclined cracks were also initiated. The majority of cracks were initiated rapidly after the yielding of the longitudinal bar. Ultimately, DBS 1 failed due to the crushing of concrete in the mid-span of the beam (hatched portion in *Fig. 5a*) after the propagation of the cracks. The cracks adjacent to the column zone then propagated in the longitudinal and transverse forms. In DBS 2 and DBS 3, cracks occurred adjacent to the side section of the drop panel and then propagated and opened at failure (alternative long and short dashed lines in *Fig. 5b and c*). This shows that the stiff drop panel with high A_{rd} influences the deterioration of the load-carrying capacity of the system due to the excessive opening of cracks adjacent to the side section of the drop panel. Therefore, A_{rd} is an important factor in determining the failure behaviour of the proposed system. Further, it should be noted that the cracks that were initiated adjacent to the side section of the drop panel (section line A–A in *Fig. 5*) tended to propagate towards the end of the rebar anchored to the slab (section line B–B in *Fig. 5*). Therefore, it can be seen that the effect of the anchorage length of the rebar on the crack propagation is significant and the selection of the anchorage length of the rebar in the drop panel is an important factor affecting the structural behaviour of DBS. In DBS 4, no prominent opening of cracks developed in the drop panel or the beam. In the design of the specimens, punching shear failure was prevented by considering the punching shear strength of the slab adjacent to the column zone, which was larger than the flexural strength corresponding to the yielding of the longitudinal reinforcement in the beam. As expected, no specimen failed in punching shear, while some cracks due to punching shear were observed until the reinforcement that crossed the critical punching shear section of the drop panel yielded

Deflections

Deflections at Service Load

Deflection is the most important factor indicating the structural performance of DBS in the gravity load resisting system. In order to study the applicability of DBS from the serviceability viewpoint, deflection at SL will be discussed in this section. *Figure 6* plots the relationship between the number of longitudinal bars and the deflection: (a) at SL; (b) at yielding of the longitudinal bar in the beam; and (c) at ultimate

state. Vertical and horizontal axes in *Fig. 6a, b and c* represent the deflection at the SL, Δ_s, and the number of longitudinal bars: (a) in the beam, A_{rb}; (b) and (c) in the drop panel, A_{rd}. The allowable deflection proposed in ACI 318-11 (l/480, where l is the span length of a beam) is also plotted in the figure.[10] The symbols, solid circles, triangles, squares and rhombuses, indicate the deflection at SL for DBS 1, DBS 2, DBS 3 and DBS 4, respectively. Also, the dashed line connecting DBS 2 and DBS 3, which have the same amount of rebar in the drop panel, $A_{rd} = 1520.4$ mm^2, is indicated in *Fig. 6a*. The deflection at SL, Δ_s, in DBS 3 was perceived to be the greatest while the values of Δ_s in DBS 1 and DBS 2 were found to be the smallest. As can be seen in the figure, the largest deflection at SL was measured for DBS 3, while the smallest deflections were attained for DBS 1 and DBS 2. A comparison between DBS 2 and DBS 3 provides the conclusion that A_{rb} influences the deflection at SL only slightly (the difference of Δ_s for DBS 2 and DBS 3 is less than 1.0 mm). It should be noted that the measured deflections at SL in all specimens were smaller than the allowable deflection, $\Delta_{allow} = 3.75$ mm. This means that the structural system proposed in this study is satisfactory for the requirement of allowable deflection, l/480, where l is the span length.

Deflection at Yielding of Longitudinal Bar in Beam and at Ultimate State

Figure 6b and c plots the relationship between the number of longitudinal bars in the drop panel, A_{rd}, and the deflection at the mid-span of the beam for each specimen at Δ_y and at Δ_u. As shown in *Fig. 6b*, an increase in A_{rd} resulted in a decrease of Δ_y. On the other hand, no correlation between A_{rd} and Δ_u was obtained, as shown in *Fig. 6c*. This is because the effective stress redistribution is caused by the value of A_{rd} in the drop panel until the longitudinal bar in the drop panel yields. Once the reinforcement in the beam yields, the contribution of the

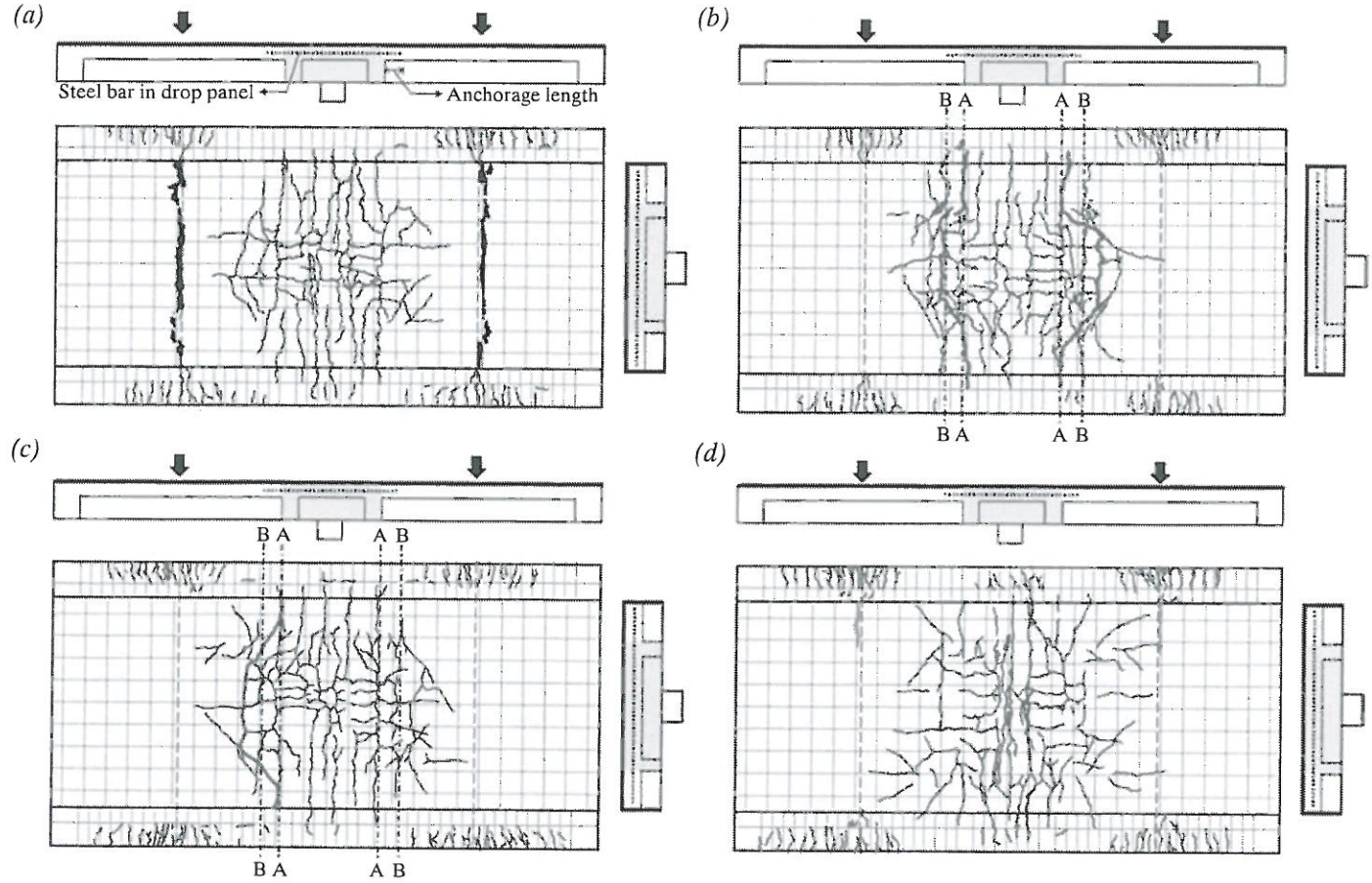

Fig. 5: Crack patterns (a) DBS 1; (b) DBS 2; (c) DBS 3; (d) DBS 4

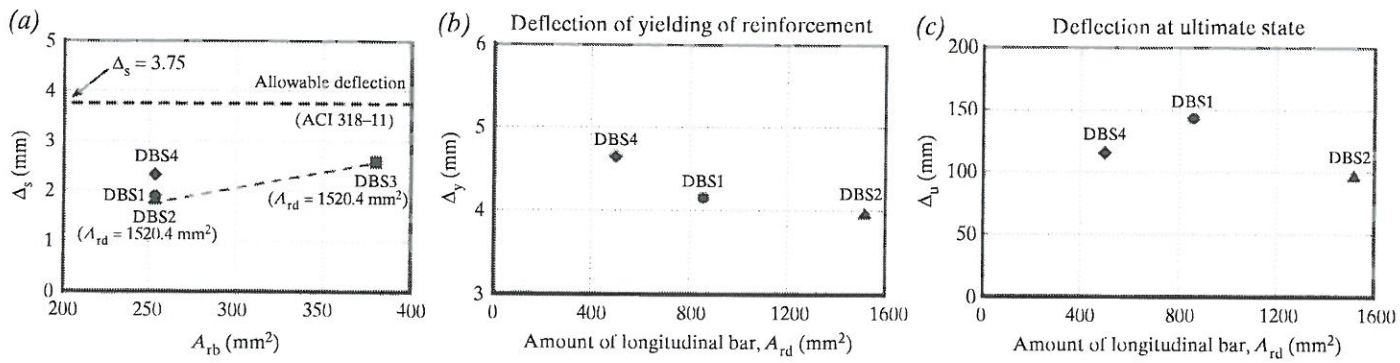

Fig. 6: Relationship between deflection and the amount of longitudinal bar. (a) At service load; (b) at yielding of rebar; (c) at ultimate state

drop panel to the external load rapidly increases and the tensile stress of the reinforcement in the drop panel also reaches its yield strength. This results in the release of stress concentration in the drop panel and uniform distribution of the stress along the drop panel to the beam. Therefore, A_{rd} and A_{rb} hardly affect the deflection at the ultimate state.

Figure 7 plots the distribution of the measured deflection in each specimen. Horizontal and vertical axes in the figure show the location at which the deflections were measured and the measured deflections, respectively. Straight bold lines in the figure indicate the deflection at SL and at Δ_y. A dashed bold line indicates the deflection at $2\Delta_y$. Straight and dashed lines in the figure represent the deflections corresponding to $4\Delta_y$ and $6\Delta_y$. As can be seen in *Fig. 7*, the deflections at the mid-span of the beams, corresponding to locations at 900 and 3600 mm along the horizontal axis, increased rapidly after Δ_y. The deflection at the critical side section of the drop panel (locations at 1800 and 2700 mm) also increased in a manner similar to that of the deflection at locations at 900 and 3600 mm. No difference in deflection at the drop panel (locations at 1800–2700 mm in *Fig. 7*) was observed for any of the specimens.

Deflection in the Drop Panel after Yielding of Longitudinal Bar

In order to quantitatively investigate how the deflections in the drop panel behave after Δ_y, a deflection ratio, Δ_{sd}/Δ_{md}, was used in this study. The ratio, Δ_{sd}/Δ_{md}, is defined as the ratio of the mean deflection at both the side sections of drop panel, Δ_{sd}, to the deflection at the mid-span of the drop panel, Δ_{md}. *Figure 8* shows the plots of Δ_{sd}/Δ_{md} versus each deflection after Δ_y for each specimen. In the figure, M_d/M_b for each specimen is also indicated. As can be seen in the figure, Δ_{sd}/Δ_{md} of a specimen with higher M_d/M_b, for instance DBS 2 (M_d/M_b = 5.19), was smaller than that of other specimens. This shows that the drop panel in DBS 2 behaved in a stiff manner due to its large number of longitudinal bars. Therefore, in order to achieve enough energy dissipation and good deformation performance, the drop panel needs to deform in an inverted U-shape and a design considering the appropriate value of M_d/M_b is required.

Reduction of Negative Moment

In DBS, placement of the drop panel at the top of the column can provide the reduction in the deflection of the beam by reduction of the negative moment in the column zone and redistribution of the moment from the mid-span of the beam to the drop panel zone. The reduction of the negative moment and redistribution of the moment in DBS can be observed from the strain distributions of the longitudinal reinforcements. *Figure 9* shows the distribution of the strain in the longitudinal reinforcements. Vertical and horizontal axes in the figure represent respectively the measured strain in the longitudinal bar and the location at which the strains were obtained. In the figure, yield lines for the reinforcements in the beam are also indicated. Similar to the case shown in *Fig. 7*, the straight bold lines are data corresponding to the SL and Δ_y. The dashed bold line indicates data for $2\Delta_y$. Straight and dashed lines represent the data at $4\Delta_y$ and $6\Delta_y$, respectively. Therefore, positive strain in the figure indicates that the specimen behaved as U-shaped. As can be seen in *Fig. 9*, the maximum tensile strains were observed at the mid-spans of the beams (locations at 900 and 3600 mm) of all specimens. Strains in the drop panel zone (locations at 1800, 2250 and 2700 mm in *Fig. 9*) were found to remain close to zero until $2\Delta_y$. It can be seen that the negative moment in the column zone was reduced effectively due to the presence of the drop panel. Also, somewhat compressive strains were measured in the mid-spans of the drop panel zones of DBS 2 and DBS 3, indicating that the drop panel deformed in an inverted U-shaped fashion. On the other hand, tensile strains were observed in the drop panel zones in DBS 2 and DBS 4 with lower A_{rd}, showing that the drop panel deformed in a U-shaped fashion. A column beneath the drop panel might not be effective at constraining the inverted U-shaped deformation of the drop panel in the case of a stiff drop panel, as shown in *Fig. 9* (DBS 2 and DBS 3), because the flexural rigidity of the drop panel with

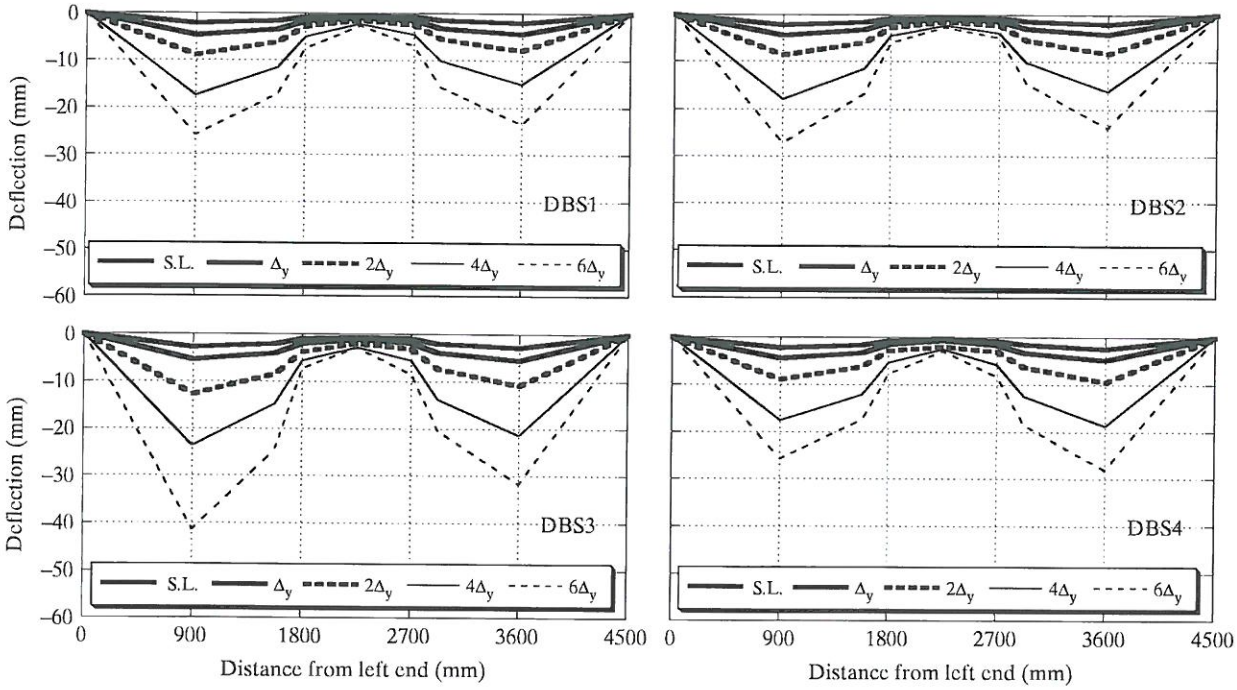

Fig. 7: Distribution of deflection of each specimen (a) DBS 1; (b) DBS 2; (c) DBS 3; (d) DBS 4

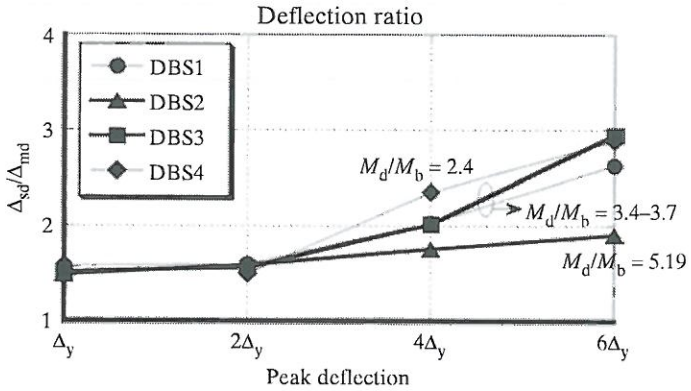

Fig. 8: Deflection after yielding of longitudinal bar (Units: [–])

higher A_{rd} is relatively greater than the axial rigidity of the column. This results in a double U-shaped deformation of the structure (DBS 2 and DBS 3). However, if a drop panel with a small number of longitudinal bars deforms in a flexible manner, a column beneath the drop panel might significantly constrain the inverted U-shaped deformation, because the axial rigidity of the column is relatively greater than the flexural rigidity of the drop panel. This results in a triple U-shaped deformation of the structure, as illustrated in *Fig. 9* (DBS 1 and DBS 4).

Decreased deflection at the mid-span of the beam after yielding (Δ_y) was also observed. It can be seen that the moment initiated at the mid-span of the beam shifted to the drop panel zone and the stress was evenly distributed in the proposed system until $6\Delta_y$. In particular, the facts that DBS 4 behaved in a ductile manner (*Fig. 4*) and that redistribution of moment happened after the yielding in DBS 4 show that local concentration of stress did not occur in DBS 4. Also, it can be seen that an A_{rd} of less than 40% of the number of steel bars in DBS 1 will be effective for the design of the proposed system. This facilitates the completion of DBS in terms of economic efficiencies.

Analysis of Economical Efficiency

Case Studies Incorporating DBS in Practice

The proposed DBS system provides economic efficiency as well as structural excellence. In this section, the economic efficiency of DBS will be scrutinized by introducing a case study incorporating DBS. DBS has been applied to structural systems of various types of buildings such as factories, family houses, hospitals, offices, parking lots, churches and apartments. As a representative case study incorporating DBS, the Y hospital building and S office building are introduced in this study. The Y hospital building is currently under construction in Gyeonggi, Korea. The building involves 13 above-ground and four below-ground floors. DBS was applied to the four below-ground floors for the parking lots of the hospital building. The floor area at each level is approximately 104 161 m^2. The RC slab has a thickness of 180 mm. The S office building is located in Daejeon, Korea. The building involve 9 above-ground and 6 below-ground floors. DBS was applied to parking lots in below-ground floors.

Cost Analysis

The material cost calculated in the structural design of the hospital building was compared with the cost of the building if it had been constructed using a conventional RC system. The structural design, using an ultimate-strength design approach that provided for the structural performance of each system, met ACI-11 code requirements[10]. *Figure 10* shows Plans A (RC system) and B (DBS) obtained for the structural design of the first basement of the hospital building. In the figure, the plan view of the first basement and the predicted specifications of the section size of the representative members in a typical unit are also indicated. The design approach

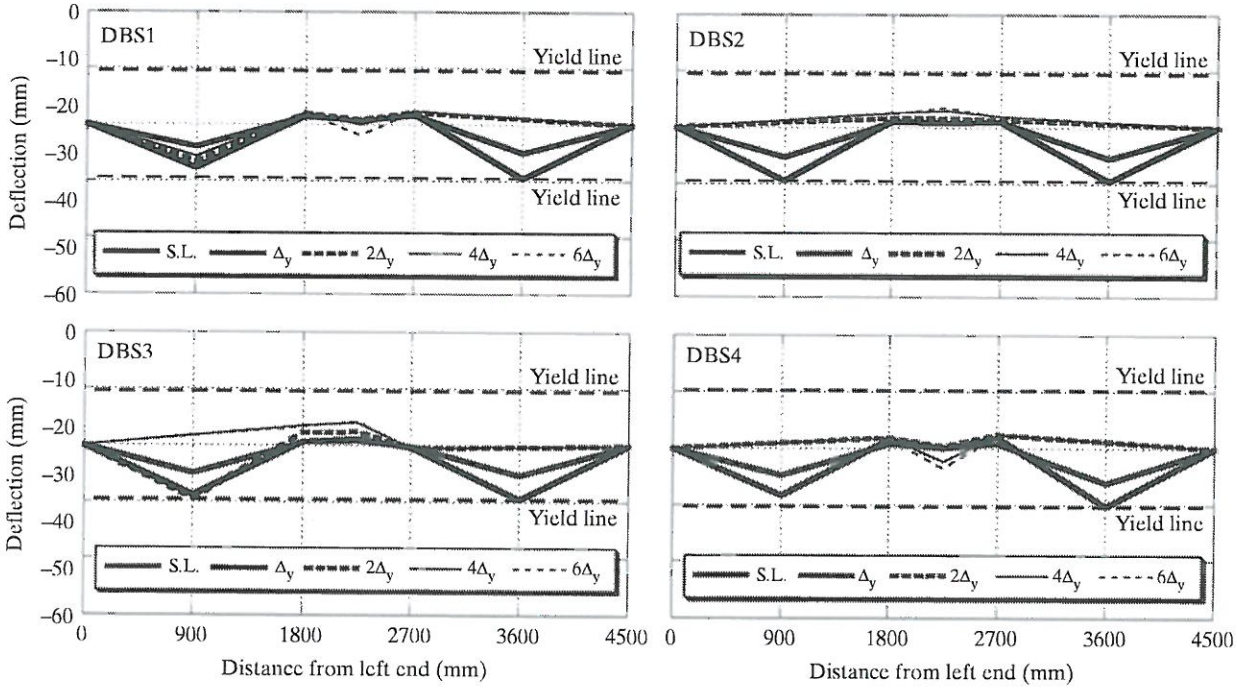

Fig. 9: Distribution of tensile strain in longitudinal bar

Materials	RC system				DBS					
	Girders		Slab		Double beams		Slab		Drop panels	
	Quantity	Cost*	Quantity	Cost*	Quantity	Cost*	Quantity	Cost*	Quantity	Cost*
Reinforcement (t)	7.5	8250	2.1	2277	2.6	2860	1.4	1540	1.2	1320
Concrete (m^3)	26.9	1883	37.2	2604	13.2	924	32.2	2254	19.0	1330
Formwork (m^2)	112.9	3161	206.6	5785	78.4	2195	179.6	5029	27.0	756
Temporary prop (m^2)	–	–	206.6	826	–	–	179.6	718	27.0	108
Sum (won)	13 294		11 492		5979		9541		3514	
	Total: 24 786 000 won = $22 627.4				Total: 19 034 000 won = $17 376.3					

*1000 won = $0.91 (as of 17 November 2014).

Table 4: Quantity comparisons between RC system and DBS for a typical unit

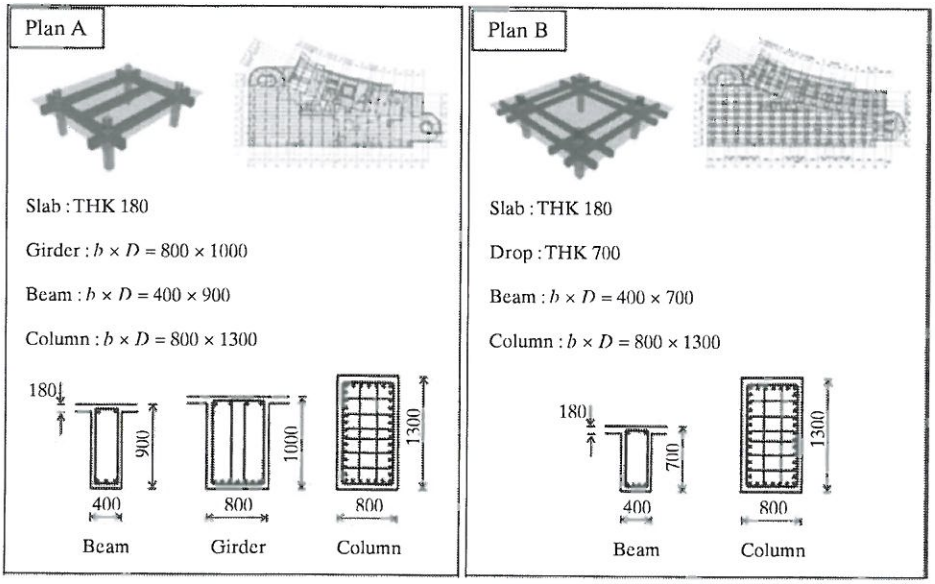

Fig. 10: Comparison of predicted material cost between RC system and DBS (Units: mm)

Buildings	MC_{RC}	MC_{DBS}	$(MC_{RC} - MC_{DBS})/MC_{RC}$ (%)
Y hospital building	$22 627.4	$17 376.3	23.2
S office building	$2 445 970.4	$1 765 211.8	27.8

Table 5: Material cost comparisons between two incorporated case studies

provided the conventional RC system with girders and beam sections of 800 mm × 1000 mm and 400 mm × 900 mm, and column sections of 800 mm × 1300 mm. For DBS, beam section of 400 mm × 700 mm and column section of 800 mm × 1100 mm were provided by the design approach. *Table 4* summarizes the parameters used to compare the RC system and DBS for a typical unit. As can be seen in the table, reinforcement weights of the RC system and DBS are 9.6 (7.5 + 2.1) and 5.2 (2.6 + 1.4 + 1.2), respectively. For the quantities of concrete, concrete volume of each system was 64.1 m3 (26.9 + 47.2) for the RC system and 64.4 m3 (13.2 + 32.2 + 19.0) for DBS, respectively. Required forms for the RC system and for DBS are 319.5 m^2 (112.9 + 206.6) and 285 m^2 (78.4 + 179.6 + 27.0), respectively. For the supporting posts in the RC system and in DBS, 206.6 m^2 is required. In summary, reinforcement weights in DBS are reduced by approximately 54%. Concrete and forms required in DBS are greater by approximately 100.6% and reduced by 89%, respectively. Quantity of supporting posts required in DBS is the same as that in the RC system. In total, a cost saving of approximately 23% is achieved for the Y hospital building by adopting DBS instead of the conventional RC system.

In the same manner, cost analysis was carried out for the other incorporated case study. *Table 5* provides a material cost comparison for each incorporated case, including that of the Y hospital building. MC_{RC} and MC_{DBS} in the table indicate respectively the material cost of the RC system and the DBS. In the table, cost savings, $(MC_{RC} - MC_{DBS})/MC_{RC}$, are also indicated. As shown in the table, cost savings of approximately 23.2%–27.8% can be achieved when DBS is applied to each building as the structural system. It can be concluded that DBS provides an approximately 25% cost-saving effect compared with the conventional RC system.

Conclusions

A new RC structural system suitable for long-span structures was developed. The system consists of a slab, a column, double beams and a drop panel. The drop panel is formed by adjacent double reinforced concrete beams penetrating to the top of the column in a #-shape. To investigate the structural performance of the system, four specimens of 30% scale were constructed and tested. In the test using two experimental parameters, the number of longitudinal bars in the beams and drop panels and the effects of the parameters on the structural behaviour of the system were scrutinized. All specimens were satisfactory in terms of the allowable deflection, *l*/480, as allowed in ACI 318-11. The drop panels of the proposed system reduced the negative moment in the column zone and contributed to effective deflection control. The system can lead to realization of long-span structures that are easy to build. Also, in the cost analysis comparing the conventional RC system with the proposed system, the advantages of the proposed system in terms of economic efficiency were confirmed. An approximately 25% cost-saving effect for the proposed system was attained.

Nomenclature

A_{rb} Number of longitudinal bars in beam

A_{rd} Number of longitudinal bars in drop panel

b Sectional width of beam or drop panel
d Effective sectional depth of beam or drop panel
E_c Young's modulus of concrete
E_s Elastic modulus of reinforcement
f_c Compressive strength of concrete
f_y Yield strength of reinforcement
f_u Tensile strength of reinforcement
h Overall section depth of beam or drop panel
l Span length
M_b Flexural strength of beam
MC_{DBS} Evaluated material cost of DBS
MC_{RC} Evaluated material cost of reinforced concrete system
M_d Flexural strength of drop panel
SL Service load
V Gravity load
V_s Gravity load at service load
V_y Gravity load at yielding of longitudinal bar
V_u Gravity load at ultimate state
Δ Deflection at mid-span of beam
Δ_{cr} Deflection at mid-span of beam corresponding to primary cracking
Δ_{md} Deflection at mid-span of drop panel
Δ_s Deflection at mid-span of beam corresponding to service load
Δ_{sd} Deflection at side section of drop panel
Δ_y Deflection at mid-span of beam corresponding to yielding of longitudinal bar in beam
Δ_u Deflection at mid-span of beam corresponding to ultimate state

Acknowledgements

This research was supported by the Functional Districts of the Science Belt support program, Ministry of Science, ICT and Future Planning (2015K000281), and by the National Research Foundation of Korea (NRF) grant funded by the Korea government (MSIP) (No. NRF-2015R1A2A2A01003397).

References

[1] Bradford MA, Gilbert RI. Composite beams with partial interaction under sustained loads. *ASCE J. Struct. Eng.* 1992; **118**(7): 1871-1883.

[2] Hicks S, Lawson RM, Lam D. Design considerations for composite beams using precast concrete slabs. Paper presented at *CCSC 2006, Proceedings of the Fifth International Conference on Composite Construction in Steel and Concrete*, Kruger National Park, South Africa, July 18–23, 2004. ASCE, 2006; 190–201.

[3] Lam D, Fu F. Behaviour of semi-rigid composite beam-column connections with steel beams and precast hollow core slabs. Paper presented at *CCSC 2006, Proceedings of the Fifth International Conference on Composite Construction in Steel and Concrete*, Kruger National Park, South Africa, July 18–23, 2004. ASCE, 2006; 443–454.

[4] Nie J, Tao M, Li S, Cai CS, Li S. Analytical and numerical modeling of prestressed continuous steel-concrete composite beams. *ASCE J. Struct. Eng.* 2011; **137**(12): 1405–1418.

[5] Nie J, Xiao Y, Tan Y, Wang H. Experimental studies on behavior of composite steel high-strength concrete beams. *ACI Struct. J.* 2004; **101**(2): 245–251.

[6] Oechlers DJ, Bradford MA. *Elementary Behaviour of Composite Steel and Composite Structural Members*. Butterworth-Heinemann: Woburn, MA, 1999.

[7] Wang Y, Yang L, Shi Y, Zhang R. Loading capacity of composite slim frame beams. *J. Construct. Steel Res.* 2009; **65**(3): 650–661.

[8] The Korea Construction Transport New-Technology Association. *Source Book of New-Technologies [in Korean]*. Public Procurement Service: Korea, 2011.

[9] MIDAS Information Technology. MIDAS Gen (Ver. 835). MIDAS Information Technology. Available from: http://www.midasuser.com.

[10] ACI Committee 318. *Building Code Requirements for Structural Concrete (ACI 318M-11) and Commentary*. American Concrete Institute: Farmington Hill, MI, 2011.